Article

Kinetics of Acid-Induced Spectral Changes in the GFPmut2 Chromophore

Stefania Abbruzzetti, Elena Grandi, Cristiano Viappiani, Sara Bologna, Barbara Campanini, Samanta Raboni, Stefano Bettati, and Andrea Mozzarelli

J. Am. Chem. Soc., **2005**, 127 (2), 626-635• DOI: 10.1021/ja045400r • Publication Date (Web): 02 December 2004

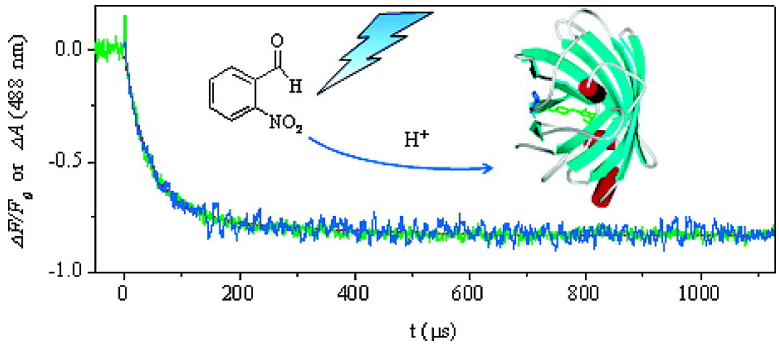

More About This Article

Additional resources and features associated with this article are available within the HTML version:

- Supporting Information
- Links to the 5 articles that cite this article, as of the time of this article download
- Access to high resolution figures
- Links to articles and content related to this article
- Copyright permission to reproduce figures and/or text from this article

View the Full Text HTML

J|A|C|S
ARTICLES
Published on Web 12/02/2004

Kinetics of Acid-Induced Spectral Changes in the GFPmut2 Chromophore

Stefania Abbruzzetti,[†,||] Elena Grandi,[†] Cristiano Viappiani,*[,†,||] Sara Bologna,[‡,||] Barbara Campanini,[‡,||] Samanta Raboni,[‡,||] Stefano Bettati,[§,||] and Andrea Mozzarelli[‡,||]

Contribution from the Dipartimento di Fisica, Università di Parma, Parco Area delle Scienze 7/A, 43100 Parma, Italy; Dipartimento di Biochimica e Biologia Molecolare, Università di Parma, Parco Area delle Scienze 23/A, 43100 Parma, Italy; Dipartimento di Sanità Pubblica, Università di Parma, via Volturno 39, 43100 Parma, Italy; and Istituto Nazionale per la Fisica della Materia, Parco Area delle Scienze 7A, 43100 Parma, Italy

Received July 30, 2004; E-mail: cristiano.viappiani@fis.unipr.it

Abstract: We have used a nanosecond pH-jump technique, coupled with simultaneous transient absorption and fluorescence emission detection, to characterize the dynamics of the acid-induced spectral changes in the GFPmut2 chromophore. Disappearance of the absorbance at 488 nm and the green fluorescence emission occurs with a thermally activated, double exponential relaxation. To understand the source of the two transients we have introduced mutations in amino acid residues that interact with the chromophore (H148G, T203V, and E222Q). Results indicate that the faster transient is associated with proton binding from the solution, while the second process, smaller in amplitude, is attributed to structural rearrangement of the amino acids surrounding the chromophore. The protonation rate shows a 3-fold increase for the H148G mutant, demonstrating that His148 plays a key role in protecting the chromophore from the solvent. The deprotonation rate for T203V is an order of magnitude smaller, showing that the hydrogen bond with the hydroxyl of Thr203 is important in stabilizing the deprotonated form of the chromophore. A kinetic model suggests that, in addition to protecting the chromophore from the solvent, His148 may act as the primary acceptor for the protons on the way to the chromophore.

Introduction

Green fluorescent protein (GFP) and its mutants are largely employed to monitor cellular processes and in a variety of biotechnological applications.[1−4] The chromophore that confers the typical color and fluorescent properties to the protein is a 4-(*p*-hydroxybenzylidene)imidazolidin-5-one originated from an internal cyclization at residues Ser65, Tyr66, and Gly67 and 1,2 dehydrogenation of Tyr66.

High-resolution crystal structures of the wild type (wt) GFP and several mutants are available (Figure 1).[1,5] The overall structure of GFP consists of an 11-stranded β-barrel with a central helix that carries the chromophore.[6,7] The X-ray diffraction and NMR studies and a variety of physicochemical methods indicate an exceptionally low conformational flexibility of the GFP fold which preserves the planar chromophore structure[7,8] and shields the chromophore from external quenchers, e.g., oxygen.[1,9,10] This feature is the basis of the reported high fluorescence quantum yield of native GFP.[2] At room temperature, denatured GFP or model chromophores in solution show no significant fluorescence due to a high conformational flexibility of the chromophore moiety.[11,12] However, when frozen in an ethanol glass at 77 K, such model compounds become highly fluorescent.[13] Inside the protein environment, the chromophore is very sensitive to mutations of surrounding residues that alter the flexibility of the chromophore, as well as its ionization state.[14]

The optical absorption and fluorescence properties of GFP are commonly explained by a three-state model[15−17] that

† Dipartimento di Fisica, Università di Parma.
‡ Dipartimento di Biochimica e Biologia Molecolare, Università di Parma.
§ Dipartimento di Sanità Pubblica, Università di Parma.
|| Istituto Nazionale per la Fisica della Materia.

(1) Zimmer, M. *Chem. Rev.* **2002**, *102*, 759−781.
(2) Tsien, R. Y. *Annu. Rev. Biochem.* **1998**, *67*, 509−544.
(3) Cubitt, A. B.; Heim, R.; Adams, S. R.; Boyd, A. E.; Gross, L. A.; Tsien, R. Y. *TIBS* **1995**, *20*, 448−455.
(4) Chalfie, M., Kain, S., Eds. *Green fluorescent protein: properties, applications and protocols*; Wiley-Liss: 1998.
(5) Labas, Y. A.; Gurskaya, N. G.; Yanushevich, Y. G.; Fradkov, A. F.; Lukyanov, K. A.; Lukyanov, S. A.; Matz, M. V. *Proc. Natl. Acad. Sci. U.S.A.* **2002**, *99*, 4256−4261.
(6) Ormö, M.; Cubitt, A. B.; Kallio, K.; Gross, L. A.; Tsien, R. Y.; Remington, S. J. *Science* **1996**, *273*, 1392−1395.
(7) Yang, F.; Moss, L. G.; G. N. P., Jr. *Nat. Biotecnol.* **1996**, *14*, 1246−1251.
(8) Striker, G.; Subramaniam, V.; Seidel, C. A. M.; Volkmer, A. *J. Phys. Chem. B* **1999**, *103*, 8612−8617.
(9) Swaminathan, R.; Hoang, C. P.; Verkman, A. S. *Biophys. J.* **1997**, *72*, 1900−1907.
(10) Ward, W. W.; Bokman, S. H. *Biochemistry* **1982**, *21*, 4535−4540.
(11) Niwa, H.; Inouye, S.; Hirano, T.; Matsuno, T.; Kojima, S.; Kubota, M.; Ohashi, M.; Tsuji, F. I. *Proc. Natl. Acad. Sci. U.S.A.* **1996**, *93*, 13617−13622.
(12) Bell, A. F.; He, X.; Wachter, R. M.; Tonge, P. J. *Biochemistry* **2000**, *39*, 4423−4431.
(13) Ward, W. W. In *Bioluminescence and Chemiluminescence: Basic Chemistry and Analytical Applications*; DeLuca, M. A., McElroy, W. D., Eds.; Academic Press: New York, 1981; pp 235−242.
(14) Kummer, A. D.; Wiehler, J.; Rehaber, H.; Kompa, C.; Steipe, B.; Michel-Beyerle, M. E. *J. Phys. Chem. B* **2000**, *104*, 4791−4798.

10.1021/ja045400r CCC: $30.25

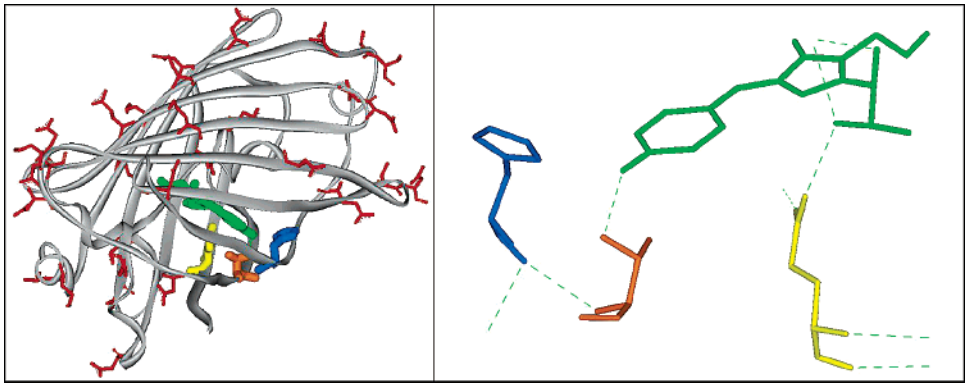

Figure 1. (Left) Three-dimensional structure of S65T GFP at pH 8 (PDB entry 1EMG). The chromophore is shown in green, His148, in blue, Thr203, in orange, and Glu222, in yellow. The carboxylic acids present on the protein are shown in red. (Right.) Closeup of the chromophore with the mutated residues.

assumes that the chromophore exists either in a protonated (band A, 395 nm) or an deprotonated (band B, 475 nm) state;[18] the latter state exists in a thermodynamically unstable intermediate form (band I, 493 nm) and a low-energy form.[19,20] The hydroxyl group of wt GFP chromophore is part of an intricate network of hydrogen bonds that favors the protonated form.[2] Deuteration experiments have shown that the large Stokes shift after excitation at 395 nm is due to excited state proton transfer of the GFP chromophore in its neutral state. After excitation the hydroxyl group of the GFP chromophore is deprotonated within a few picoseconds and a predominant red-shifted fluorescence emission from the deprotonated chromophore is observed. At room temperature this emission is spectrally not distinguishable from emission upon 475 nm excitation.[15,16] The phenolic hydroxyl of the chromophore is hydrogen bonded through a water molecule to Ser205, which is also hydrogen bonded to the γ-carboxylate of Glu222. Electrostatic repulsion in this network between the γ-carboxylate of Glu222 and the phenolic chromophore has been proposed to stabilize the protonated state of the chromophore.[17,21]

Though wt GFP is relatively insensitive to changes in pH,[22] the fluorescence emission of several GFP mutants exhibits distinct pH dependences.[1,2] Among others, mutations involving Ser65 are of special interest since they lead to the selective stabilization of the deprotonated form, shifting the pK_a around neutrality.[2] The most commonly used mutation to favor ionization of the phenol of the chromophore is the replacement of Ser65 by Thr (S65T),[23] though several other aliphatic residues such as Gly, Ala, Cys, and Leu have roughly similar effects (class 2 mutants).[2,23−25] Based on crystallographic studies it was assumed that in the S65T mutant the chromophore is fully deprotonated at pH 8 (Figure 1) and protonated at pH 4.5.[26] Furthermore, Glu222 is not in hydrogen-bonding contact with the phenolate oxygen of the chromophore, showing that, for this mutant, Glu222 is not able to stabilize the protonated state of the chromophore.[6] Fluorescence excitation spectra of S65T showed that for this mutant the absorbance band A does not lead to appreciable fluorescence emission.[27,28]

Since the initial proposal for the use of a GFP mutant as a reporter of the pH within cellular compartments,[29] several studies have described the pH sensitivity of other GFP variants[27,30−33] and the use of these variants as endogenous intracellular pH indicators.[27,31]

A detailed kinetic description of the pH-induced transformations at the chromophore site is desirable not only for the understanding of the mechanisms underlying the change in color but also for the evaluation of how fast the protein can respond to changes in pH. Stopped flow pH-jump measurements, carried out to study the kinetics of the acid-induced transformation of the chromophore in the S65T GFP, demonstrated that the spectral changes occurred within the instrumental dead time (about 2 ms).[27] Fluorescence correlation spectroscopy (FCS) has been recently used to monitor pH-dependent fluctuations in EGFP (F64L-S65T) and S65T GFP.[28] The autocorrelation function was described as arising from a decay with pH-dependent rate, which was attributed to binding of protons from solution, and a slower, pH-independent process, assigned to an intramolecular proton transfer and/or structural rearrangement. Similar findings were reported for YFP mutants.[34] Although FCS is an extremely powerful tool to investigate dynamic events in macromolecules, relaxation methods have some advantages since they require minimal modeling to retrieve kinetic informa-

(15) Chattoraj, M.; King, B. A.; Bublitz, G. U.; Boxer, S. G. *Proc. Natl. Acad. Sci. U.S.A.* **1996**, *93*, 8362−8367.
(16) Lossau, H.; Kummer, A.; Heinecke, R.; Pollinger-Dammer, F.; Kompa, C.; Bieser, G.; Jonsson, T.; Silva, C. M.; Yang, M. M.; Youvan, D. C.; Michel-Beyerle, M. E. *Chem. Phys.* **1996**, *213*, 1−16.
(17) Brejc, K.; Sixma, T. K.; Kitts, P. A.; Kain, S. R.; Tsien, R. Y.; Ormo, M.; Remington, S. J. *Proc. Natl. Acad. Sci. U.S.A.* **1997**, *94*, 2306−2311.
(18) Heim, R.; Prasher, D. C.; Tsien, R. Y. *Proc. Natl. Acad. Sci. U.S.A.* **1994**, *91*, 12501−12504.
(19) Creemers, T. M. H.; Lock, A. J.; Subramaniam, V.; Jovin, T. M.; Volker, S. *Proc. Natl. Acad. Sci. U.S.A.* **2000**, *97*, 2974−2978.
(20) Creemers, T. M. H.; Lock, A. J.; Subramaniam, V.; Jovin, T. M.; Völker, S. *Nat. Struct. Biol.* **1999**, *6*, 557−560.
(21) Palm, G. J.; Zdanov, A.; Gaitanaris, G. A.; Stauber, R.; Pavlakis, G. N.; Wlodawer, A. *Nat. Struct. Biol.* **1997**, *4*, 361−365.
(22) Ward, W. W.; Prentice, H. J.; Roth, A. F.; Cody, C. W.; Reeves, S. C. *Photochem. Photobiol.* **1998**, *31*, 803−808.
(23) Heim, R.; Cubitt, A. B.; Tsien, R. Y. *Nature* **1995**, *373*, 663−664.
(24) Delagrave, S.; Hawtin, R. E.; Silva, C. M.; Yang, M. M.; Youvan, D. C. *Bio-Technology* **1995**, *13*, 151−154.
(25) Cormack, B. C.; Valdivia, R. H.; Falkow, S. *Gene* **1996**, *173*, 33−38.
(26) Elsliger, M. A.; Wachter, R. M.; Hanson, G. T.; Kallio, K.; Remington, S. J. *Biochemistry* **1999**, *38*, 5296−5301.
(27) Kneen, M.; Farinas, J.; Li, Y.; Verkman, S. *Biophys. J.* **1998**, *74*, 1591−1599.
(28) Haupts, U.; Maiti, S.; Schwille, P.; Webb, W. W. *Proc. Natl. Acad. Sci. U.S.A.* **1998**, *95*, 13573−13578.
(29) Wachter, R. M.; King, B. A.; Heim, R.; Kallio, K.; Tsien, R. Y.; Boxer, S. G.; Remington, S. J. *Biochemistry* **1997**, *36*, 9759−9765.
(30) Wachter, R. M.; Elsliger, M. A.; Kallio, K.; Hanson, G. T.; Remington, S. J. *Structure* **1998**, *6*, 1267−1277.
(31) Llopis, J.; Mccaffery, J. M.; Miyawaki, A.; Farquhar, M. G.; Tsien, R. Y. *Proc. Natl. Acad. Sci. U.S.A.* **1998**, *95*, 6803−6808.
(32) Miesenbock, G.; Angelis, D. A. D.; Rothman, J. E. *Nature* **1998**, *394*, 192−195.
(33) Robey, R. B.; Ruiz, O.; Santos, A. V. P.; Ma, J.; Kear, F.; Wang, L.; Li, C.; Bernardo, A. A.; Arruda, J. A. L. *Biochemistry* **1998**, *37*, 9894−9901.
(34) Schwille, P.; Kummer, S.; Heikal, A. A.; Moerner, W. E.; Webb, W. W. *Proc. Natl. Acad. Sci. U.S.A.* **2000**, *97*, 151−156.

tion. We have used a nanosecond pH-jump technique, coupled with simultaneous transient absorption and fluorescence emission detection, to gain insight into the dynamics of the structural changes at the chromophore moiety for a GFP class 2 mutant. The absorbance and emission properties of the triple mutant S65A, V68L, and S72A, called GFPmut2,[25] were previously characterized.[35] While showing very similar spectroscopic features to those of S65T,[25,35] GFPmut2 offers some advantages, like higher folding and chromophore formation efficiencies at 37 °C.[25] The pH dependence of the absorbance and the fluorescence emission of GFPmut2 exhibited an identical pK_a of 6.1 ± 0.1, indicating that only the protonated and unprotonated forms, absorbing at 380 and 485 nm, respectively, are in equilibrium.[35] Following the initial finding that the conversion of the deprotonated form of the chromophore occurrs with kinetics in the microsecond range,[36] we have undertaken a detailed characterization of this process. To understand the source of the observed kinetic events, selected amino acids were mutated (H148G, T203V, and E222Q; see Figure 1), and the relaxation kinetics after the nanosecond pH-jump was characterized.

Materials and Methods

Protein Expression. A GFPmut2 gene was subcloned from pKEN2 vector[25,37] into a modified version of the His-tagged expression vector pET28b(+) (Novagen) using *Cpo*I restriction site. The pET28*Cpo*I:: GFPmut2 construct was sequenced and used for the transformation of BL21(DE3) cells (Novagen).

All mutants were obtained from the wild-type construct using the Quikchange site-directed mutagenesis kit (Stratagene). Oligonucleotides were synthesized by MWG-Biotech.

Protein expression was induced with 1 mM isopropyl-β-D-thiogalactopyranoside (Sigma) to a mid-logarithmic growth phase cell culture in Luria-Bertani broth. Crude extract was loaded onto a Talon metal affinity column (CLONTECH), and GFP was then eluted with a 150 mM imidazole-containing buffer. After proteolitic treatment with thrombin (15 units per mg of protein) the protein was purified from the undigested His-tagged protein and the cleaved His-tagged peptides by metal affinity chromatography. Sample purity was assessed by SDS-PAGE analysis and determined to be 99%. Protein stocks were stored at −80 °C. The S65T mutant was a kind gift of V. Subramaniam (Max Planck Institute for Biophysical Chemistry, Göttingen, Germany).

Steady-State Spectroscopy. Green fluorescent proteins from stock solutions were diluted in 10 mM citrate−100 mM phosphate buffer at different pH's, ranging from 4.5 to 8.6.[38] Steady-state fluorescence spectra were acquired with a FluoroMax-3 spectrofluorometer (Jobin Yvon Horiba). Protein concentration was 0.1 μM. Absorption spectra were collected with a Cary400 spectrophotometer. Protein concentration was 2 μM. The sample compartment temperature was mantained at 25 °C. The pH of each sample was controlled after the measurement.

The pH dependence of the absorbance or fluorescence emission was used to estimate the pK_a of the conversion from the deprotonated to the protonated forms of the GFP samples, using an equation derived from a simple ionization equilibrium:[39]

$$y = a + (b - a)\frac{10^{n(\mathrm{p}K_a - \mathrm{pH})}}{1 + 10^{n(\mathrm{p}K_a - \mathrm{pH})}} \quad (1)$$

where y is either the absorbance or the fluorescence emission (excitation) intensity at selected wavelengths, a and b are the values of the parameter at acidic and alkaline pH values, and n is an empirical Hill coefficient.

Nanosecond pH-Jump Setup. The nanosecond pH-jump was obtained by photolysis of the caged proton 2-NBA.[40,41] Photoexcitation of an aqueous solution of *2*-NBA with a 355 nm nanosecond laser pulse leads to the release of protons in high yield ($\Phi_{H^+} = 0.45$), within a few nanoseconds.[40,42−44] The concentration of photoreleased protons can reach the 10^{-4} M range with laser pulses of a few tens of mJ.[45,46] At low laser pulse energies, the concentration of photoreleased protons is proportional to the laser pulse energy. At each laser pulse energy, the concentration of photoreleased protons can be calculated from the protonation rate (determined through the absorbance changes) of a suitable pH indicator.[41,47] For the setup used in the reported experiments, the molar concentration of photoreleased protons available for reactions with binding sites on the protein can be calculated as $[H^+]_0(M) = 5.0 \times 10^{-6}E$, where E is the energy of the laser pulses expressed in mJ.

The single-shot, laser flash photolysis setup for transient absorption was described previously.[45] The fluorescence emission from the protein was excited at 488 nm with a cw Ar^+ laser (Uniphase), which served also as the light source for the transient absorption. The green fluorescence emission was collected from the bottom of the quartz cuvette with a compact photomultiplier (Hamamatsu, H6780) in front of which suitable filters were positioned. In particular, two dichroic mirrors were cascaded, the first with a high reflectivity at 355 nm (>99%, CVI) to remove the stray light from the pump laser and the second to select the fluorescence emission and reject the 488 nm excitation (514−560 nm, Omega Optics). The current output of the photomultiplier was converted to a voltage and amplified by a home-built, DC-coupled broadband amplifier (100 MHz). The voltage signals from the APD and the photomultiplier were fed into the two input channels of a digital sampling oscilloscope (LeCroy 9370, 1 GHz, 1 Gs/s). To avoid bleaching, the samples were exposed to the intense 488 nm light only during the time necessary for data acquisition, using a fast mechanical shutter (Uniblitz). Temperature was controlled by a peltier element with a feedback control mounted below the cuvette holder. This allowed temperature stability of better than 0.1 °C to be achieved in the temperature range 10−50 °C. To allow for collection of the fluorescence emission from the bottom of the cuvette, a peltier element with a center hole was employed. Dry gas flowing on the sample holder prevented condensation of humidity on the cuvette walls. The absorbance of 2-nitrobenzaldehyde (2-NBA) at 355 nm was kept at 2, while the absorbance of GFP samples was on the order of 0.07−0.1 at 488 nm. The main advantage of this setup is that it allows simultaneous collection of absorbance and fluorescence emission data, with single shot sensitivity.

The time resolution of the setup is limited by the laser pulse width for the transient absorbance detection, while it is limited to ∼1 μs for the fluorescence emission, due to the intense spike generated by the pulsed laser (vide infra).

(35) Chirico, G.; Cannone, F.; Beretta, S.; Diaspro, A.; Campanini, B.; Bettati, S.; Ruotolo, R.; Mozzarelli, A. *Protein Sci.* **2002**, *11*, 1152−1161.
(36) Viappiani, C.; Abbruzzetti, S.; Bologna, S.; Campanini, B.; Bettati, S.; Mozzarelli, A. *Biophys. J.* **2003**, *84*, 341A.
(37) Ezaz-Nikpay, K.; Uchino, K.; Lerner, R. E.; Verdine, G. L. *Protein Sci.* **1994**, *3*, 132−138.
(38) McIlvaine, T. C. *J. Biol. Chem.* **1921**, *49*, 183−186.
(39) Marshall, A. G. *Biophysical Chemistry: Principles, Techniques and Applications*; John Wiley and Sons: New York, Brisbane, Toronto, Chichester, 1978.
(40) Bonetti, G.; Vecli, A.; Viappiani, C. *Chem. Phys. Lett.* **1997**, *269*, 268−273.
(41) Viappiani, C.; Bonetti, G.; Carcelli, M.; Ferrari, F.; Sternieri, A. *Rev. Sci. Instrum.* **1998**, *69*, 270−276.
(42) George, M. V.; Scaiano, J. C. *J. Phys. Chem.* **1980**, *84*, 492−495.
(43) Carcelli, M.; Pelagatti, P.; Viappiani, C. *Isr. J. Chem.* **1998**, *38*, 213−221.
(44) Abbruzzetti, S.; Carcelli, M.; Rogolino, D.; Viappiani, C. *Photochem. Photobiol. Sci.* **2003**, *2*, 796−800.
(45) Abbruzzetti, S.; Viappiani, C.; Small, J. R.; Libertini, L. J.; Small, E. W. *J. Am. Chem. Soc.* **2001**, *123*, 6649−6653.
(46) Abbruzzetti, S.; Sottini, S.; Carcelli, M.; Viappiani, C. Submitted.
(47) Gutman, M.; D.Huppert; E. Pines *J. Am. Chem. Soc.* **1981**, *103*, 3709−3713.

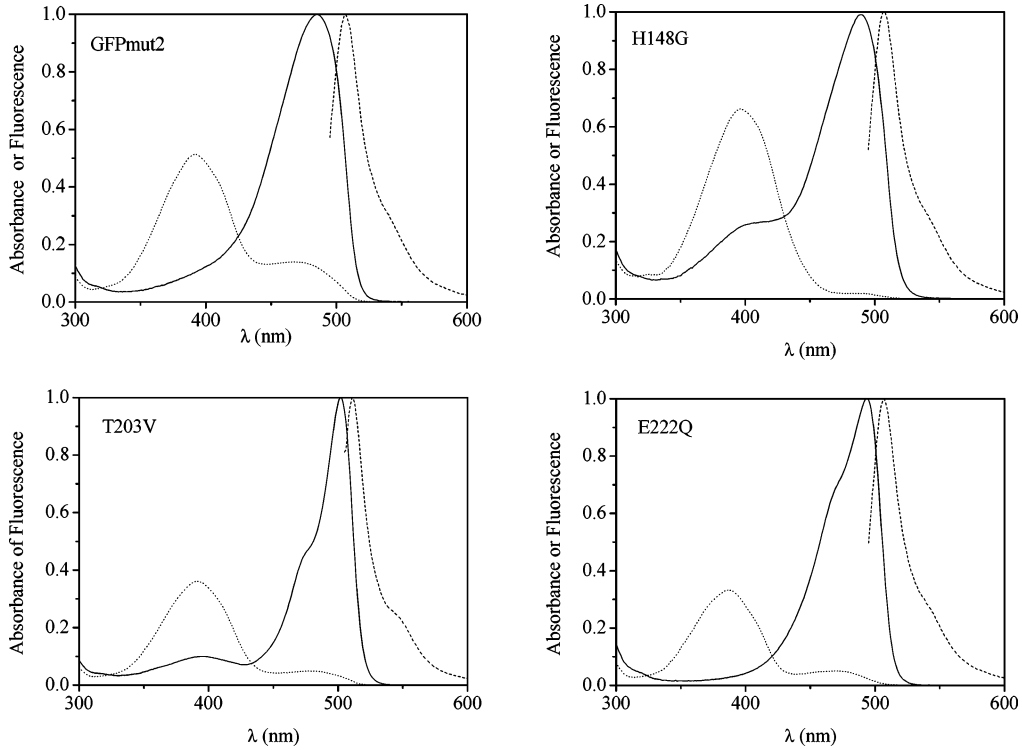

Figure 2. Comparison between the absorbance spectra (solid lines) and the fluorescence emission spectra (dashed line) of the deprotonated forms of GFPmut2 and the investigated mutants. The absorbance spectra of the protonated forms are reported as dotted lines. The excitation wavelength for the emission spectrum was 485 nm. Spectra were measured at pH 4.9 and pH 8.4 for GFPmut2, pH 5.5 and pH 8.8 for H148G, pH 4.5 and pH 8 for T203V, and pH 4.3 and pH 8.0 for E222Q.

To retrieve kinetic information, fluorescence emission (F) was converted to relative change with respect to prepulse value (F_0) by taking the ratio:

$$\frac{\Delta F}{F_0} = \frac{F - F_0}{F_0} \tag{2}$$

Kinetic traces of ΔA or $\Delta F/F_0$ were fitted with a sum of two exponential decay functions using Origin 7.0 (OriginLab).

Results

Spectral Properties of Selected Mutants as a Function of pH. The fluorescence emission spectrum of the alkaline form (pH = 8.4) of GFPmut2 has a peak at 507 nm.[25,35] The corresponding absorption spectrum shows a band centered at 485 nm (band B). Lowering the pH to 4.9 results in 90% decrease of the absorbance intensity. A similar behavior is observed for the fluorescence emission. Below pH 8.4 an absorbance peak at 393 nm appears (band A) and increases substantially on lowering the pH of the solution. Excitation at this wavelength leads to a very weak fluorescence emission with a spectrum similar to the one recorded after 485 nm excitation.

The pH-dependent changes in fluorescence emission closely parallel absorbance changes, indicating that GFPmut2 molar absorbance rather than fluorescence quantum yield changes with pH. Further support to this comes from the fluorescence lifetimes. At pH 7 and after excitation at 485 nm the fluorescence emission is characterized by a double exponential decay with lifetimes 3.3 ns (84%) and 1.0 ns (16%).[35] The values are essentially unaffected by pH in the investigated range, thus confirming the independence of the fluorescence quantum yield from pH (data not shown). This behavior closely resembles the properties of GFP S65T.[27]

Table 1. Summary of Parameters for GFPmut2 and the Investigated Mutants

	λ_{abs} (nm)	pK_a	λ_{em} (nm)	pK_a
GFPmut2	485	6.12 ± 0.01	507	6.16 ± 0.03
H148G	488	7.57 ± 0.02	507	7.26 ± 0.02
T203V	502	6.21 ± 0.02	511	6.21 ± 0.03
E222Q	494	6.0 ± 0.1	506	6.14 ± 0.05

Far-UV circular dichroism experiments showed that the observed changes with pH of the spectral properties of GFPmut2 are not correlated with changes in the secondary structure of the protein, as already observed for S65T (data not shown).[26−28]

The absorbance and fluorescence emission spectra as well as their pH dependence were found to vary in the mutants H148G, T203V, and E222Q (Figure 2). The position and the shape of the absorbance band in the visible spectral range (band B) is shifted for all mutants with respect to GFPmut2 (Table 1). On the contrary, the transition in the near-UV is scarcely affected by the mutations, with observed changes of less than 2 nm. The fluorescence emission maximum appears to be substantially red-shifted only for T203V. While the shape of the low energy peak (band B) for GFPmut2 is characteristic for a structureless electronic transition, this band exhibits clear vibrational features for T203V and E222Q, and, less evident, also for H148G. In particular, evident shoulders are noticeable at ∼475 nm. These features suggest that these mutations introduce some additional rigidity in the chromophore environment, as also suggested by the increased specularity of the fluorescence emission and absorbance bands.

The absorbance spectra of the acidic form of the chromophore of the mutants shown in Figure 2 indicate that in all cases the absorbance band B is converted to the absorbance band A when

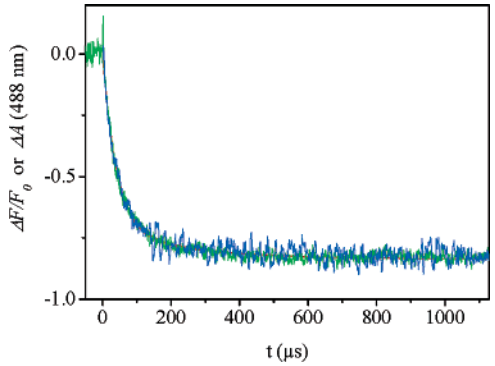

Figure 3. Changes in absorbance at 488 nm (blue) and in the fluorescence emission (green) following a single 355 nm, 30 mJ laser pulse for an aqueous solution containing 2-NBA (2 mM) and GFPmut2 (1 μM) at $T = 30$ °C, with a prepulse pH of 7.5. The laser pulse energy corresponds to $[H^+]_0 = 150\ \mu$M. The fitting with a double exponential relaxation (red curves) yields $\tau_1 = 40 \pm 3\ \mu$s (86 ± 5%), $\tau_2 = 230 \pm 20\ \mu$s (14 ± 5%). Absorbance changes were normalized to the relative fluorescence changes to show the perfect overlap of the two curves.

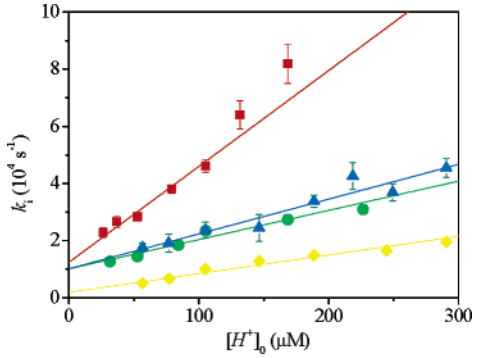

Figure 4. Rate constants k_1 for GFPmut2 (green circles), H148G (red squares), T203V (yellow diamonds), and E222Q (blue triangles) as a function of $[H^+]_0$ at $T = 20$ °C. The solid lines are the fits with straight lines to the k_1 data.

Table 2. Protonation and Deprotonation Rate Constants for the Investigated Samples

	k_{1p} (10^8 M^{-1} s^{-1})	k_{1d} (10^3 s^{-1})	k_2 (10^3 s^{-1})
GFPmut2	1.08 ± 0.02	10 ± 1	2.1 ± 0.6
H148G	3.3 ± 0.2	12 ± 2	3 ± 1
T203V	0.65 ± 0.05	1.9 ± 0.1	1.0 ± 0.2
E222Q	1.1 ± 0.1	11 ± 1	2 ± 2

pH is lowered. Table 1 also reports the pK_a determined by the analysis of the sigmoidal curves obtained by plotting the maximum absorbance as a function of pH (data not shown). In all cases, the transition is well described by proton binding to a single site (or to several sites with the same binding constant) with $n = 1$ (eq 1).[39] The pK_a is substantially affected only by mutation at His148. Titration curves for the fluorescence emission give pK_a values identical to those determined from absorbance data, except for H148G (Table 1). In this case, the pK_a determined from the fluorescence emission was 0.3 units lower than the value obtained from absorbance spectra, suggesting a more acidic character of the excited state. A detailed characterization of the photophysical properties of the mutants is beyond the scope of this work and will be reported elsewhere.

Kinetics of Acid-Induced Changes of the Spectral Properties of the Chromophore. When an aqueous solution of 2-NBA and GFPmut2 is flashed with a single, 355 nm laser pulse, both the absorbance at 488 nm and the fluorescence emission decrease (Figure 3), as expected on the basis of the equilibrium data (Figure 2). The changes in absorbance or fluorescence occur on the microsecond time scale, and no further variation is observed at longer time scales. Control experiments indicated that no signal was detectable in the absence of 2-NBA, apart from a fluorescence spike at short times, due to the excitation of the GFP chromophore by the intense 355 nm light. In addition, no appreciable bleaching of the chromophore due to the 355 nm pulse was evident from the analysis of the traces. This indicates that the observed kinetics can be associated with the change in pH of the solution and discards possible photoreactions of the GFP chromophore.

Within the laser pulse energy range we have used, the concentration of protons $[H^+]_0$ is always much larger (>25 μM) than the reacting chromophore concentration (~1 μM). This qualifies the reaction between photodetached protons and the chromophore as pseudo-first-order. Hence, the relaxation kinetics associated with binding of protons to the chromophore can be approximated by exponential decay functions.

In all of the experiments we invariably found that the fluorescence emission and the absorbance respond to the laser induced pH-jump with identical kinetics. The relaxation kinetics can be described under all conditions by a double exponential decay function with the same lifetimes for the absorbance and fluorescence emission. Therefore, fittings were performed on fluorescence and absorbance kinetic traces, taken under the same experimental conditions, with lifetimes as shared parameters. From the lifetimes τ_1 and τ_2, apparent rates can be determined as $k_1 = 1/\tau_1$ and $k_2 = 1/\tau_2$.

Increasing the laser pulse energy results in faster kinetics. However, only the rate k_1 is actually affected by the concentration of photoreleased protons. This rate increases linearly with $[H^+]_0$ (Figure 4) with a slope $k_{1p} = (1.08 \pm 0.02) \times 10^8$ M^{-1} s^{-1} and an intercept $k_{1d} = (10 \pm 1) \times 10^3$ s^{-1} for GFPmut2 at 20 °C. Under pseudo-first-order conditions, k_{1p} can be interpreted as the protonation rate while k_{1d} represents the deprotonation rate. The rate k_2 of the slower process is essentially constant with an average value of $(2.1 \pm 0.6) \times 10^3$ s^{-1} in the laser pulse energy range we have investigated. Similar findings were obtained with all investigated mutants, with rates differing in their absolute values. The slopes and the intercepts are summarized in Table 2.

Control experiments with S65T showed that the conversion from the deprotonated to the protonated form occurs with biexponential kinetics at 20 °C (data not shown). The rate k_1 increases with $[H^+]_0$, while k_2 ($(1.6 \pm 0.7) \times 10^3$ s^{-1}) is not affected by this parameter. The rates k_{1p} and k_{1d} for S65T are $(1.1 \pm 0.4) \times 10^8$ M^{-1} s^{-1} and $(4 \pm 2) \times 10^3$ s^{-1}, respectively.

The kinetic response of the absorbance and the fluorescence emission was found to be temperature dependent. To determine the activation parameters we have systematically investigated, at several temperatures, the absorbance and fluorescence emission kinetics in response to the laser pH-jump at a single laser pulse energy (i.e., at a single $[H^+]_0$). Fitting of the experimental traces with two exponential decay functions gave satisfactory results at all investigated temperatures. Figure 5 shows Arrhenius plots for the rate constants measured for GFPmut2. The Arrhenius plots for k_1 were linear and gave very similar activation energies for the investigated samples. The activation

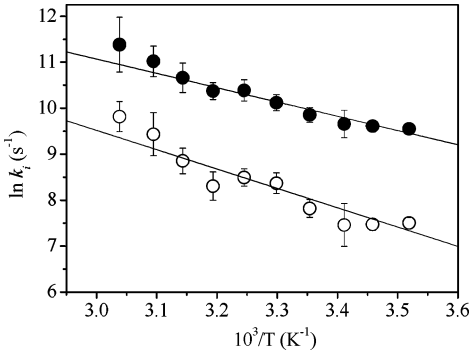

Figure 5. Arrhenius plot for the rate constants determined from the kinetics of the acid-induced transformation of the chromophore in GFPmut2 (1 μM) after photolysis of 2-NBA (2 mM). Filled symbols refer to k_1, and open symbols refer to k_2. Data were measured with a laser pulse energy of 30 mJ at a prepulse pH of 7.2. The laser pulse energy corresponds to $[H^+]_0 =$ 150 μM.

Table 3. Activation Parameters for the Investigated Mutants

	E_{a1} (kcal mol^{-1})	ln(k^0_1) (s^{-1})	E_{a2} (kcal mol^{-1})	ln(k^0_2) (s^{-1})
GFPmut2	6.2 ± 0.6	20.4 ± 0.2	8.3 ± 0.2	22.1 ± 0.3
H148G	7.1 ± 0.6	23 ± 1	8.4 ± 0.4	22.8 ± 0.6
T203V	8.2 ± 0.1	23.6 ± 0.1	13.2 ± 0.3	29.6 ± 0.4
E222Q	6.3 ± 0.8	21 ± 1		

energies obtained from k_2 showed some variations in response to mutations. In particular, the barrier for the T203V mutant was substantially higher than that for GFPmut2, while for E222Q the barrier was negligible. These parameters are summarized in Table 3.

The first process is characterized by an activation barrier significantly higher than that reported for diffusion of free protons in water, which was estimated to be ~2.5 kcal/mol at room temperature.[48] An alternative estimate for the diffusional barrier has been given as 4.3 kcal/mol.[49] Our results indicate that protons have to pass a substantially higher energy barrier than the normal diffusional barrier to reach the binding site on the phenolate. This value is consistent with diffusion-mediated binding of protons to reaction sites embedded in proteins as apomyoglobin[50] and polypeptides.[51] The barrier for binding of H^+ to a single fluorescein covalently attached to Bacteriorhodopsin was found to be 8.4 kcal/mol.[52] This value was interpreted as arising from the existence of several protonation/deprotonation reactions with amino acid side chains.

The activation barrier for the diffusion mediated binding of protons (E_{a1}) is scarcely, if at all, influenced by the mutations. Some effects of the mutations were noticed on the activation barrier for the second process (E_{a2}). Removal of Thr203 and substitution with a Val residue increase substantially the energetic barrier associated with this process. Mutation of Glu222 has an opposite effect, although the lack of a detectable energetic barrier for E222Q must be taken only as indicative, since for this sample problems were encountered due to its tendency to aggregate.

Discussion

The kinetics of the conversion of the deprotonated form of the chromophore to its conjugate acid following the nanosecond acidification of the solution is equally sensed by the absorbance at 488 nm and the fluorescence emission, excited at 488 nm (Figure 3). Therefore, the measured kinetics reflects the conversion of the ground-state deprotonated form to the ground-state protonated form of the chromophore.

The apparent rate constant k_1 of the shortest lived decay increases with laser pulse energy (i.e., with the concentration of photoreleased protons) for all investigated samples. This indicates that the faster transient is related to diffusion-mediated proton binding to an acceptor, affecting the optical properties of the chromophore. However, the k_{1p} protonation rates, reported in Table 2, are much smaller than those reported for diffusion-mediated processes. Previous determinations of the rate constant for proton binding to several residues in proteins indicate that their value is invariably found in the 10^9-10^{10} M^{-1} s^{-1} range.[50,53,54] The unusually low value for k_{1p} suggests that the access of protons to the chromophore is restricted. This finding is consistent with the position of the chromophore, which is located in the interior of the protein barrel, shielded from the solvent. Indeed, fluorescence quenching experiments have shown that this location provides a good protection against quenching by several agents, e.g., oxygen, and attack by hydronium ions.[1,9,10] The value of k_{1p} for GFPmut2 is essentially identical to the value determined for the S65T mutant, showing that the accessibility of the chromophore to the solvent is very similar for both proteins. On the contrary, the deprotonation rate k_{1d} is 2-fold lower. The low value of the protonation rate suggests that there is no efficient proton-transfer mechanism at work between acidic primary acceptors (carboxylates) and the chromophore.[55,56] The large distance between the acidic groups and the chromophore (Figure 1) is evidently at the source of this low efficiency.

The accessibility of the chromophore to the solvent is strictly correlated with structural fluctuations in the β-can region in the proximity of the phenolic moiety. For several regions, including the first α-helix and β-sheets 3, 7, 8, and 10, increased hydrogen−deuterium exchange rates were taken as suggestions for a substantial conformational flexibility on the microsecond to millisecond time scales usually attributed to hydrogen bonds being broken. In crystal structures of GFPs, a reduced interstrand hydrogen bonding network can be observed for β-strands 7, 8, and 10. This may be caused either by dynamic conformational processes or by inefficient side chain packing inside the GFP β-barrel which leads to diverging β-strands and, therefore, larger interstrand distances.[57] The importance of dynamical processes around β-strand 7 emerges from several indications. According to molecular dynamics simulations, conformational fluctuations occur in the cleft between β-sheets 7 and 8, mainly connected to flipping of the Arg168 side chain[58] at least on a nanosecond time scale. ^{19}F NMR studies on the cyan variant of GFP showed

(48) Agmon, N. *Isr. J. Chem.* **1999**, *39*, 493−502.
(49) Yoshino, A.; Yoshido, T.; Takahashi, K. *Magn. Reson. Chem.* **1989**, *27*, 344−347.
(50) Abbruzzetti, S.; Crema, E.; Masino, L.; Vecli, A.; Viappiani, C.; Small, J. R.; Libertini, L. J.; Small, E. W. *Biophys. J.* **2000**, *78*, 405−415.
(51) Abbruzzetti, S.; Viappiani, C.; Small, J. R.; Libertini, L. J.; Small, E. W. *Biophys. J.* **2000**, *79*, 2714−2721.
(52) Heberle, J.; Dencher, N. A. *Proc. Natl. Acad. Sci. U.S.A.* **1992**, *89*, 5996−6000.
(53) Gutman, M.; Nachliel, E. *Biochim. Biophys. Acta* **1990**, *1015*, 391−414.
(54) Marantz, Y.; Nachliel, E. *Isr. J. Chem.* **1999**, *39*, 439−445.
(55) Yam, R.; Nachliel, E.; Gutman, M. *J. Am. Chem. Soc.* **1988**, *110*, 2636−2640.
(56) Gutman, M.; Nachliel, E. *Ann. Rev. Phys. Chem.* **1997**, *48*, 329−356.
(57) Seifert, M. H. J.; Georgescu, J.; Ksiazek, D.; Smialowski, P.; Rehm, T.; Steipe, B.; Holak, T. A. *Biochemistry* **2003**, *42*, 2500−2512.
(58) Helms, V.; Straatsma, T. P.; McCammon, J. A. *J. Phys. Chem. B* **1999**, *103*, 3263−3269.

that His148 is likely to be involved in a slow exchange process.[59] These fluctuations likely allow protons to diffuse into the protein matrix through entry channels which open transiently.

Besides being modulated by the fluctuations of the barrel, the accessibility of the chromophore to the protons coming from the bulk is likely to be mediated by some primary acceptor. The most probable candidate is His148. Suggestions about the existence of some primary acceptor come also from the pK_a values determined from the forward and reverse rate constants in Table 2, which differ substantially from the equilibrium values reported in Table 1.

The activation energies of the reactions (see E_{a1} values in Table 3) also suggest that the protonation of the chromophore is not direct but rather mediated by some intermediate process having a much higher activation energy than that of pure water. This intermediate could be identified either in a protonation step on the proton-transfer pathway or in the fluctuations of the barrel leading to transient opening of the can.

The second process detected in our experiments exhibits a lifetime of ~500 μs, at 20 °C, for GFPmut2. This lifetime is independent of the extent of the pH-jump. There are several possible sources for this process: (i) it could reflect a proton transfer from a primary acceptor to the final protonation site; (ii) it may be associated with a structural relaxation of the protein matrix around the chromophore in response to the protonation of the phenolate; (iii) it may arise from the slow conversion of the protonated ground state to a dark state. The last two hypotheses cannot be distinguished on the basis of our experiment, and further analysis, possibly at the single molecule level, may be necessary to properly interpret the underlying mechanism. The lifetime of this transient is compatible with the pH-independent fluctuations measured with FCS for S65T, EGFP, and two yellow mutated proteins.[28,34] The authors proposed that the fluctuations might be associated with dynamics of the barrel in the region close to the chromophore, modulating its accessibility to the solvent. It was suggested a possible involvement of His148 in shuttling protons from the exterior to the interior of the protein. Recent NMR experiments detected fluctuations in the strands 7−10, with a characteristic time similar to that determined from FCS data.[57,59] Our data for S65T can be compared with the previously reported FCS results.[28] Although the deprotonation rate estimated by FCS (9.05×10^3 s^{-1}) appears to be in line with our determination, the protonation rate estimated by FCS (3.45×10^9 M^{-1} s^{-1}) is much higher than the value we have determined.

Our data can also be compared to those recently reported for a similar laser pH-jump experiment on S65T.[60] In that work the authors reported that conversion of the deprotonated form of GFP S65T occurs with a monoexponential relaxation, whose lifetime depends on the viscosity of the solution. Our findings clearly show that, for GFPmut2 and for S65T, a double exponential kinetics is observed under all the investigated conditions. In that work, no transient absorbance data were reported, and protonation and deprotonation rates were not determined. The lack of a second component is probably due to the limited time resolution and sensitivity of the instrumental apparatus used in that work, which prevented access to times shorter than 20 μs.

Although it is not possible to obtain the protonation rate from the data reported by Mallik et al.,[60] the apparent lifetime of 87 μs following the laser pH-jump in the absence of glycerol is consistent with our determination and much lower than the value obtained from FCS on the same sample. At this stage it is not clear why the rates determined by FCS are so much higher than the value determined with the laser pH-jump method.

Effect of Mutations on Rate Constants. The mutations at key sites of the protein have some effects on the observed kinetics. When His148 is substituted with Gly, the protonation rate k_{1p} shows a remarkable increase (Table 2). This finding shows that in this mutant the chromophore has a higher direct accessibility to the solvent. On the other hand, the deprotonation rate remains unaffected. The straightforward interpretation of this effect is that substitution of the imidazole with a less bulky aliphatic group creates a hole in the β-can, thus allowing an easier entrance way for the protons coming from the solvent. The value of k_{1p} is almost identical for GFPmut2, T203V, E222Q, and S65T GFP, showing that while His148 is a key residue in shielding the chromophore from the bulk solvent, all other mutations do not alter the path of the protons to the chromophore. His148 is directly hydrogen bonded to the phenolic end of the chromophore in the high pH S65T structure (Figure 1)[26] and in YFP,[30] and it was proposed to constitute a protective barrier between the chromophore and bulk solvent.[26] This residue is relatively solvent exposed but exhibits a lower pK_a, suggested to be below 5 in both S65T and YFP, in comparison with a free His.[26] In both the low and high pH structures of S65T, the imidazole proton can be assigned to $N_{\delta 1}$, since this nitrogen is a hydrogen bond donor to the backbone oxygen of Asn146 at pH 4.6 and to the chromophore phenolate at pH 8.0. The imidazole $N_{\epsilon 1}$ is a hydrogen bond acceptor from the backbone nitrogen of Arg168 in both cases, providing a rationale for the apparently lowered pK_a of His148 as compared to a free His. NMR experiments have reported direct evidence for the existence of a slow exchange process, with a characteristic time of ~1 ms, between two different conformational states of CFP, suggesting that His148 may modulate the accessibility of the chromophore to the solvent.[57,59] An entropy/enthalpy compensation was observed for this process, and an activation energy of 14 kcal/mol was estimated from temperature-dependent experiments.[59] The influence of His148 on the accessibility of the chromophore to the solvent has both static and dynamic origins. The mutation of His148 to Gly in YFP causes a larger β-strand separation between the backbones of residues 148 and 168.[30] The side chain of Ile167 is relocated toward the space previously occupied by the imidazole ring. In GFP, β-strands 7 and 8 are connected by a hydrogen bond between His148 N_ϵ and Arg168 N. In the wild-type crystal structure,[7] Arg168-folds over His148. Therefore, removal of His148 is supposed to destabilize the protein barrel, leading to more pronounced conformational fluctuations. In addition, direct solvent access to the chromophore was found to be greatly improved by the H148G mutation of YFP.[30] Finally, mutations at positions 147, 149, 164−168, 202, and 220 (located in β-strands 7, 8, 10, and 11) have been shown to increase the pH sensitivity of the GFP chromophore.[32] This effect is supposed

(59) Seifert, M. H. J.; Ksiazek, D.; Azim, M. K.; Smialowski, P.; Budisa, N.; Holak, T. A. *J. Am. Chem. Soc.* **2002**, *124*, 7932−7942.
(60) Mallik, R.; Udgaonkar, J. B.; Krishnamoorthy, G. *Proc. Indian Acad. Sci. (Chem. Sci.)* **2003**, *115*, 307−317.

to be caused by an increased conformational flexibility around the chromophore.

Although all these arguments support the idea that His148 may act as a shield from the solvent, they do not disprove a role for this residue as a mediator in the proton pathway from the exterior to the chromophore. This aspect will be discussed below.

The only effect on the deprotonation rate k_{1d} is observed for T203V mutant (Table 2). The deprotonation rate is five times lower than the corresponding values for the other mutants. There are a few reports on the spectroscopic phenomenology of nonaromatic T203 mutants of GFP. Two similar T203I mutants were shown to shift the chromophore ground-state equilibrium toward the protonated state.[18,61] Owing to the missing hydroxyl group of T203, there is less stabilization of the deprotonated form and the corresponding absorption band is almost entirely lost. Another variant containing T203I in a multiple mutation environment exhibited both absorbance bands A and B, the latter red-shifted to 507 nm.[62] This large red shift was assumed not to arise from any of the single mutations alone but rather from a cooperative effect. More recently, the effects of Thr203 replacement with both aliphatic and aromatic residues were systematically investigated.[14]

Replacing T203 with the isosteric Val leads to a pronounced red shift (502 nm) of the steady-state absorption band of the deprotonated form of the chromophore in GFPmut2 (485 nm). A similar effect was reported for this substitution into wt GFP, for which a consistent red shift was observed in the steady-state absorption band of the deprotonated form of the chromophore, which amounted to 77% of the one achieved by Tyr substitution.[14] Although the recent X-ray structure for the mutant T203Y/S65G/V68L/S72A revealed $\pi-\pi$-stacking between Y203 and the tyrosyl moiety of the chromophore,[30] the large red shift in the case of aliphatic substitutions at position 203 indicates that $\pi-\pi$-stacking is not the sole origin of this effect. It is interesting to note that cooperative effects brought about by multiple mutations[21] are not responsible for the red shift, since this shift also occurs after single-site mutations. Structural investigations by Brejc et al.[17] lead to the conclusion that in wt GFP the deprotonated species of the chromophore is stabilized by a strong hydrogen bond network around the chromophore tyrosyl group including a hydrogen bond to the hydroxyl group of T203. This OH group is missing in the mutants T203V, I, F, H or remote from the phenolic oxygen of the chromophore in T203Y. Therefore, the deprotonated form cannot be stabilized[14] and the ground-state equilibrium is shifted toward the protonated chromophore, providing a structural basis for the strong decrease in the deprotonation rate that we have observed for the T203V mutant of GFPmut2.

Kinetic Model for the Protonation Reaction of GFP Chromophore. Our findings suggest for His148 an obvious role as a shield from the solvent. However, we have already suggested that, in addition to this evident effect, His148 may be involved in the primary binding of protons from the bulk at rates of $\sim 10^{10}$ M^{-1} s^{-1}. The protonated residue may then be able to shuttle protons to the less acidic phenolic oxygen of the chromophore. This could possibly explain the observed low protonation rate of the chromophore. The removal of His148, besides opening a hole in the β-can, thus facilitating the entrance of protons from the bulk, could actually decrease the rate of the binding step from the bulk, by removal of the primary acceptor. To explore the consistency of this mechanism we derived a kinetic model, starting from that originally proposed by Yam et al.[55] When protons are released to the solution, they undergo diffusion mediated reactions with the acceptors. If complex polyelectrolytes as proteins are present, the combination of a number of reactions determines the distribution of protons among surface groups of the macromolecule.[55,56] The side chains carrying groups with acidic character, such as carboxylates, bind very quickly protons from the bulk and may shuttle them to those groups characterized by higher pK_a.[52,56,63−65] The analysis of proton binding to macromolecular structures, carried out on several different proteins, invariably afforded rate constants in a range characteristic of diffusion-controlled reactions, i.e., $(2-6) \times 10^{10}$ M^{-1} s^{-1}.[56] The intrinsic rate constant for protonation of solvent exposed His residues is about 5×10^9 M^{-1} s^{-1}, identical to the average value for Lys residues of BSA and lysosyme.[53−56] A similar value was reported for protonation of Lys residues inside poly-L-lysine.[66] Solvent exposed Tyr can bind protons with a rate of 2×10^{10} M^{-1} s^{-1}.[56] Protonation of carboxylates occurs with rates between 10^{10} M^{-1} s^{-1} and 6×10^{10} M^{-1} s^{-1}, depending on the specific protein environment.[51,53,54]

A solution to the intricate problem of determining the rate constant for proton transfer to a final acceptor has been proposed by Gutman and co-workers several years ago when analyzing the problem of proton distribution between primary acceptors and the monitored chromophores.[55] During kinetic analysis of the proton-binding dynamics to surface groups, the exchange of protons between them is quantitated by a virtual second-order rate constant that is suitable for comparison between various systems.[67,68] The exchange rate is the key factor in determining the rate at which protons are transferred to the final acceptor, which is the monitored chromophore.

The structure of GFP is such that all of the primary acidic acceptors (Glu and Asp residues) are solvent exposed and far from the only entrance site through the barrel available to protons, located in the proximity of His148 (Figure 1). The only Glu residue close to the chromophore is Glu222, which is located in the interior of the protein. Similar considerations apply to His residues. However, His148 is treated separately to evidence its possible role as the primary proton acceptor. Direct protonation of His148 and exchange reactions with the other reactants have been included explicitly. This primary binding step is of course missing in the H148G mutant and the related eqs 5, 6, 9, and 11 have been accordingly neglected. Given the prepulse pH values (see Table 4), reactions 15 through 18 have been considered only for the H148G mutant. In any case, reactions with hydroxide have very little influence on the observed kinetics, given the low concentration of OH^-.

(61) Ehrig, T.; O'Kane, D. J.; Prendergast, F. G. *FEBS Lett.* **1995**, *367*, 163−166.
(62) Palm, G. J.; Wlodawer, A. *Methods Enzymol.* **1999**, *302*, 378.
(63) Heberle, J.; Riesle, J.; Thiedemann, G.; Oesterhelt, D.; Dencher, N. A. *Nature* **1994**, *370*, 379−382.
(64) Alexiev, U.; Marti, T.; Heyn, M. P.; Khorana, H. G.; Scherrer, P. *Biochemistry* **1994**, *33*, 13693−13699.
(65) Scherrer, P.; Alexiev, U.; Marti, T.; Khorana, H. G.; Heyn, M. P. *Biochemistry* **1994**, *33*, 13684−13692.
(66) Viappiani, C.; Abbruzzetti, S.; Small, J. R.; Libertini, L. J.; Small, E. W. *Biophys. Chem.* **1998**, *73*, 13−22.
(67) Gutman, M.; Nachliel, E. *Biochim. Biophys. Acta* **1995**, *1231*, 123−138.
(68) Shimoni, E.; Nachliel, E.; Gutman, M. *Biophys. J.* **1993**, *64*, 480−483.

The proton-transfer processes were then modeled according to the following scheme:

$$2\text{-NBA} \xrightarrow{h\nu} \text{NBA}^- + \text{H}^+ \quad (3)$$

$$\text{Chro}^- + \text{H}^+ \underset{k_{-1}}{\overset{k_1}{\rightleftharpoons}} \text{ChroH} \quad (4)$$

$$\text{His}_{148} + \text{H}^+ \underset{k_{-2}}{\overset{k_2}{\rightleftharpoons}} \text{HHis}_{148}^+ \quad (5)$$

$$\text{ChroH} + \text{His}_{148} \underset{k_{-3}}{\overset{k_3}{\rightleftharpoons}} \text{Chro}^- + \text{HHis}_{148}^+ \quad (6)$$

$$\text{RCOO}^- + \text{H}^+ \underset{k_{-4}}{\overset{k_4}{\rightleftharpoons}} \text{RCOOH} \quad (7)$$

$$\text{ChroH} + \text{RCOO}^- \underset{k_{-5}}{\overset{k_5}{\rightleftharpoons}} \text{Chro}^- + \text{RCOOH} \quad (8)$$

$$\text{RCOOH} + \text{His}_{148} \underset{k_{-6}}{\overset{k_6}{\rightleftharpoons}} \text{RCOO}^- + \text{HHis}_{148}^+ \quad (9)$$

$$\text{His} + \text{H}^+ \underset{k_{-7}}{\overset{k_7}{\rightleftharpoons}} \text{HHis}^+ \quad (10)$$

$$\text{HHis}^+ + \text{His}_{148} \underset{k_{-8}}{\overset{k_8}{\rightleftharpoons}} \text{His} + \text{HHis}_{148}^+ \quad (11)$$

$$\text{HHis}^+ + \text{Chro}^- \underset{k_{-9}}{\overset{k_9}{\rightleftharpoons}} \text{His} + \text{ChroH} \quad (12)$$

$$\text{HHis}^+ + \text{RCOO}^- \underset{k_{-10}}{\overset{k_{10}}{\rightleftharpoons}} \text{His} + \text{COOH} \quad (13)$$

$$\text{ChroH} \xrightarrow{k_{11}} \text{ChroH}^* \quad (14)$$

$$\text{OH}^- + \text{H}^+ \underset{k_{-12}}{\overset{k_{12}}{\rightleftharpoons}} \text{H}_2\text{O} \quad (15)$$

$$\text{ChroH} + \text{OH}^- \underset{k_{-13}}{\overset{k_{13}}{\rightleftharpoons}} \text{Chro}^- + \text{H}_2\text{O} \quad (16)$$

$$\text{RCOOH} + \text{OH}^- \underset{k_{-14}}{\overset{k_{14}}{\rightleftharpoons}} \text{RCOO}^- + \text{H}_2\text{O} \quad (17)$$

$$\text{HHis}^+ + \text{OH}^- \underset{k_{-15}}{\overset{k_{15}}{\rightleftharpoons}} \text{His} + \text{H}_2\text{O} \quad (18)$$

The formation of the nitronic acid ($pK_a = 2.1 \pm 0.2$[43,44]) occurs on a subnanosecond time scale,[69−71] and the deprotonation rate of this acidic intermediate is in the 10^8 s^{-1} range.[44] The change in concentration of free protons (eq 3) is therefore treated as instantaneous and is accordingly introduced as an initial condition $[H^+]_0$. Formation of the final photoproduct nitrosobenzoic acid occurs within a few nanoseconds from photoexcitation[42,44] and is considered instantaneous. The reaction with lysines has been neglected, since at the prepulse pH values of our experiments (between 7 and 8.2) these residues are all protonated and do not contribute to the observed kinetics.

Table 4. Parameters Obtained from the Fitting of the Numerical Solution of the Differential Equations to the Experimental Data, $T = 20$ °C

rate constants		GFPmut2	T203V	E222Q	H148G
k_1 (10^6 M^{-1} s^{-1})	$Chro^- + H^+$	0.99	0.10	1.0	300
k_2 (10^9 M^{-1} s^{-1})	$His_{148} + H^+$	5.0	5.0	4.9	
pK_a(His148)		5.35	5.40	5.49	
k_{-3} (10^{10} M^{-1} s^{-1})[b]	$HHis_{148}^+ + Chro^-$	2.9	1.3	4.2	
k_4 (10^{10} M^{-1} s^{-1})	$RCOO^- + H^+$	5.4	5.4	5.4	5.4
k_{-5} (10^9 M^{-1} s^{-1})[b]	$Chro^- + RCOOH$	0.4	0.4	1.3	1.8
k_6 (10^9 M^{-1} s^{-1})	$RCOOH + His_{148}$	1	1	1	
k_7 (10^9 M^{-1} s^{-1})	His+ H^+	6.3	6.2	6.2	5.5
k_8 (10^7 M^{-1} s^{-1})*	$HHis^+ + His_{148}$	8.5	8.6	8.5	
k_9 (10^2 M^{-1} s^{-1})*	$HHis^+ + Chro^-$	6.1	130	0.97	0.88
k_{-10} (10^9 M^{-1} s^{-1})	His + RCOOH	1.0	1.0	1.0	1.1
k_{11} (10^3 s^{-1})		1.2	0.45	1.4	0.93
k_{-13} (M^{-1} s^{-1})[a§]	$Chro^- + H_2O$				0.19
k_{14} (10^9 M^{-1} s^{-1})	$RCOOH + OH^-$				1
k_{15} (10^5 M^{-1} s^{-1})[a]	$HHis^+ + OH^-$				9
$[H^+]_0$ (μM)		81	70	80	62
prepulse pH		7.5	7.2	7.0	8.2

[a] Very little dependence on these parameters was observed, and their value is accordingly to be considered only as indicative of a low exchange rate.[55] [b] The fitting was performed on the forward rate constants. The reverse rates reported in the table are obtained from the forward rates and the pK_a of the reactions.

To properly account for the stoichiometry of the reactions, the concentrations of the reactants RCOOH and His have been obtained from the protein concentration by scaling it with factors corresponding to the number of reacting sites on the protein. In the sequence we can identify 32 "reacting" carboxylates (32 between Asp and Glu, plus the carboxy terminal), neglecting the contribution from Glu222 which is hidden. Ten His residues are present in the sequence of GFPmut2. Out of these, three are hidden from the solvent. Therefore, a total of seven residues (one of which is His148) are expected to contribute to the observed kinetics. The pK_a's of the chromophore in the different mutants were set to the values derived from the equilibrium measurements (Table 1).

We wish to point out that the rates we retrieve with our model represent averaged values over the ensemble of reactive sites on the protein and cannot be assigned to specific sites. The only rates attributable to specific groups are those referring to His148 and to the chromophore.

Numerical solutions to the set of coupled differential equations describing the coupled reactions 3−18 were determined by using the function ODE15S within Matlab. The numerical solution of the set depends on several rate constants, as well as on the concentration of the photodetached protons, $[H^+]_0$, proportional to the laser pulse energy and the initial concentration of the various reactants. To take into account a possible structural relaxation, reaction 14 was added and included in the fitting algorithm as an additional exponential decay. Some of these rate constants were left free to vary, while others were fixed to values already available from the literature.[53,55,56] Along with the concentration of photoreleased protons, and the initial concentration of protein, these parameters were optimized using a nonlinear fitting algorithm, namely a Matlab version of the optimization package Minuit, CERN. Reverse reaction rate constants have been introduced in the differential equations using the known pK_a values for the reactions.[53]

The optimization of the numerical solution of the set of coupled differential equations associated with the kinetic model allows the determination of the microscopic rate constants. To

(69) Yip, R. W.; Sharma, D. K.; Giasson, R.; Gravel, D. *J. Phys. Chem.* **1984**, *88*, 5770−5772.
(70) Yip, R. W.; Sharma, D. K.; Giasson, R.; Gravel, D. *J. Phys. Chem.* **1985**, *89*, 5328−5330.
(71) Yip, R. W.; Wen, Y. X.; Gravel, D.; Giasson, R.; Sharma, D. K. *J. Phys. Chem.* **1991**, *95*, 6078−6081.

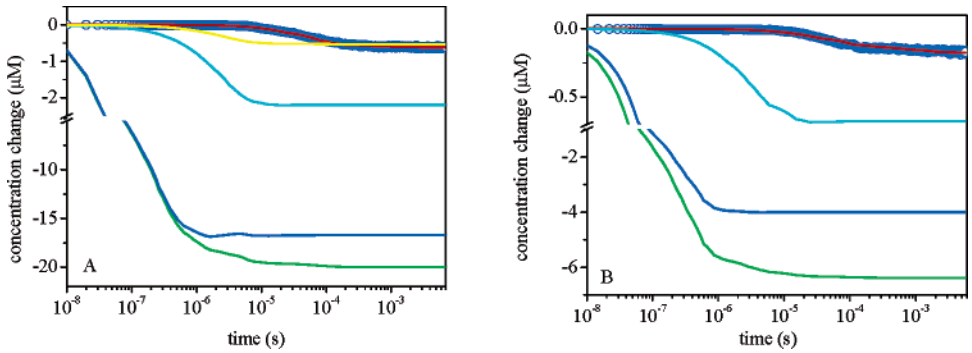

Figure 6. Fit of the time course of changes in [Chro$^-$] (open blue circles) in μM units for GFPmut2 (left) and H148G (right). The red line is the fit to the concentration change, the cyan line is the time course of changes in [His], the solid blue line is the time course of changes in [RCOO$^-$], and the green line is the time course of the proton concentration change. The yellow line in panel A is the change in [His_{148}]. The samples included 2-NBA to give an absorbance at 355 nm of 1 cm^{-1} and GFPmut2 (0.57 μM) or H148G (0.14 μM). Prepulse pH was 7.5 for GFPmut2 and 8.2 for H148G. $[H^+]_0$ was 81 μM for GFPmut2 and 62 μM for H148G. $T = 20$ °C.

improve the reliability of the retrieved parameters we have performed simultaneous fits of several curves measured at different laser pulse energy values at constant temperature. The complexity of the parametric fit prevented retrieving reliable kinetic parameters as a function of temperature. Further refinements of the method and acquisition of signals with better signal/noise ratio may allow us to perform also this analysis. Figure 6 shows the result of the fit to experimental curves for GFPmut2 and H148G. Analogous fits were obtained for the other mutants. As expected, protonation of carboxylates and His residues leads to a substantial buffering of photoreleased protons. Table 4 summarizes the relevant parameters obtained from this analysis. The relaxation rate k_{11} is in agreement with the k_2 data in Table 2. It is important to observe that the exchange rates between primary acceptors (Glu, Asp, and His) and the chromophore (k_{-5} and k_9) are invariably low and the direct transfer of protons from these acceptors to the phenolate occurs with low yield.[54−56] Binding rates to carboxylates (k_4) agree with previous determinations of this parameter.[51,53,54] The pK_a retrieved for His148 is around 5.4 in all the mutants, in agreement with the expectations that this residue has a more acidic character than solvent exposed His.[26] Protons are bound by this residue with a rate of $\sim 5 \times 10^9$ M^{-1} s^{-1}, a value which is in keeping with the literature.[53−56] After binding to His148, protons are shuttled to the phenolate anion with rates exceeding 10^{10} M^{-1} s^{-1}, which can be considered as indicative of an efficient transfer.[54−56]

Although the complex system of differential equations does not allow us to obtain the parameters with very high precision, it clearly reproduces the observed kinetics with rate constants supporting a role of His148 as the primary acceptor. This is of course not a final proof of the mechanism, but it definitely shows the likeliness of the hypothesis.

It is also important to observe that, besides acting as the primary proton acceptor, His148 also acts as a shield to the solvent, as evidenced by parameter k_1. Removal of this residue in H148G leads to a remarkable increase in k_1, showing that the direct interaction of the protons entering from the bulk with the phenolate oxyanion is strongly enhanced. Inclusion of the intermediate protonation step in the kinetic model naturally evidences the double role of His148, which modulates the chromophore accessibility to the solvent and acts as a proton carrier to the phenolic oxygen of the chromophore. Further refinements of the model and, possibly, the improvement in signal detection may allow the determination of the temperature dependence of the microscopic rate constants. This will help in understanding the reason of the apparently similar activation energy for process k_{1p} in the investigated mutants.

Conclusions

The response of the GFPmut2 chromophore to a rapid change in pH occurs with a complex kinetics reflecting a diffusion mediated binding of protons to the phenolate anion and a subsequent process likely due to the rearrangement of the local hydrogen bond network surrounding the chromophore. The protons react with the phenolate with a very low reaction rate, reflecting the protection exerted by the protein fold on the chromophore. The accessibility is strongly enhanced after removal of His148, demonstrating that this residue screens the chromophore against diffusing reactants, in agreement with earlier structural information. The attribution of this binding step to the reaction with the phenolate is substantiated also by the data for T203V, showing that substitution of the hydroxyl with a methyl group leads to a stabilization of the protonated state of the chromophore.

Besides confirming the involvement of His148 in modulating the accessibility of the chromophore to the solvent, a kinetic model allows us to attribute an additional role to His148, which appears to act as the primary acceptor for protons coming from the bulk. Protons are then shuttled to the phenolic oxyanion of the chromophore with relatively high efficiency.

Acknowledgment. The authors acknowledge INFM and MIUR (FIRB Nanotechnologies) for financial support. Centro Interfacoltà Misure of the University of Parma is acknowledged for the use of the circular dichroism facility. One of the reviewers is acknowledged for suggestions which led to a substantial improvement of the kinetic model.

JA045400R